PHOTOION–PHOTOELECTRON COINCIDENCE SPECTROSCOPY OF THE TRANSIENT MOLECULES SO AND S_2O

K. NORWOOD [1] and C.Y. NG
Ames Laboratory, US Department of Energy [2]
and Department of Chemistry, Iowa State University, Ames, IA 50011, USA

Received 13 January 1989; in final form 22 February 1989

Photoion–photoelectron coincidence (PIPECO) spectra, in the wavelength range of 1025–1210 Å, for SO and S_2O formed in a microwave discharge of SO_2 have been measured using a pulsed PIPECO method. Vibronic bands attributable to the formation of $SO^+(\tilde{X}\,^2\Pi_{3/2,1/2}, v=0\text{–}11)$, $S_2O^+(X\,^2A', v'=0\text{–}2)$, and $S_2O^+(^2A', ^2A'', v'=0\text{–}3)$ are resolved in the SO^+ and S_2O^+ PIPECO spectra. The spin–orbit splitting for $SO^+(\tilde{X}\,^2\Pi)$ is determined to be 371 ± 20 cm^{-1}. The ionization energies for SO and S_2O obtained from photoionization efficiency measurements are 10.294 ± 0.004 eV (1204.4 ± 0.5 Å) and 10.584 ± 0.005 eV (1171.4 ± 0.5 Å), respectively. The pulsed PIPECO method used in this experiment is superior in both sensitivity and resolution compared to the continuous multichannel scaling PIPECO scheme.

1. Introduction

Photoelectron spectroscopic measurements have provided most of the energetic information available today on molecular cations in their ground and excited states [1,2]. Combined with high level quantum calculations, photoelectron spectroscopic studies also yield structural information on molecular ions. Due to the difficulty in the preparation of radicals, the photoelectron spectroscopic study of radicals remains in its infancy. The reactive nature of radicals usually prevents the production of radicals with high purity. However, many radicals can be produced readily in electrical discharge, photodissociation, and thermal pyrolysis sources, coexisting with their precursors and products resulting from secondary reactions. In order to measure unambiguously the photoelectron spectrum (PES) of a specific radical formed in such a source, an experimental method capable of identifying the origins of photoelectrons, must be used. The photoion–photoelectron coincidence (PIPECO) techniques measure the time-correlated electron–ion pairs formed in photoionization and is most suitable for measuring PESs of radicals coexisting with other molecular species. To our knowledge, the application of PIPECO techniques to the study of transient species [#1] has not been made previously.

In an effort to provide thermochemical data for radicals and transient molecules relevant to combustion chemistry, we have developed a pulsed PIPECO method for radical studies. In this communication, we present preliminary results on the PIPECO study of SO and S_2O. Both SO and S_2O are products of the combustion of sulfur at low oxygen pressures [4].

2. Experimental

The experimental arrangement of the PIPECO apparatus has been described previously [5–7]. Briefly, the apparatus consists of a 3 m near normal inci-

[1] Hansen Research Fellow.

[2] Operated for the US Department of Energy by Iowa State University under Contract No. W-7405-Eng-82. This work was supported by the Director for Energy Research, Office of Basic Energy Sciences.

[#1] A transient molecule is defined to have a lifetime less than a few minutes in the pressure range of 0.1–1 Torr encountered in its production [3].

0 009-2614/89/$ 03.50

dence vacuum ultraviolet (VUV) monochromator, a capillary discharge lamp, a VUV light detector, a microwave discharge source for radical production, a quadrupole mass spectrometer (QMS) for ion detection, and an electron energy analyzer for threshold photoelectron (TPE) detection.

The transient molecules SO and S_2O, together with other gaseous species, are produced by a low pressure microwave discharge of pure SO_2 in a quartz tube. The gaseous mixture formed by the discharge flows into a buffer chamber which is evacuated by a 6″ liquid-nitrogen-trapped diffusion pump system. A small fraction of the gases enters the photoionization region as an effusive beam through a 3 mm × 1.5 mm slit between the buffer and photoionization chambers. During the experiment, the buffer and photoionization chambers are maintained at 2×10^{-4} and 2.5×10^{-5} Torr, respectively. Photoionization efficiency (PIE) measurements show that SO_2, SO, S_2O, S_3, S_2, S, O, O_2, and SO_3 are major constituents of the effusive beam. The intensity of SO_2^+ is greater than those of other ions by at least a factor of five.

The energy resolution for the detection of TPEs depends strongly on the electrostatic field at the photoionization region. In this experiment, the photoionization region is kept nearly field free. The coincidence detection is initiated by an electronic pulse signifying the arrival of a TPE at the electron detector. The electronic pulse triggers two identical extraction pulses, which have a width (Δt) of 100 ns and a height of 300 V, to extract photoions toward the ion detector. The QMS is used to select the ion of interest for detection. The first and second extraction pulses are delayed by 0 and 40 μs, respectively, with respect to the electronic pulse. Since the electron flight time from the photoionization region to the electron detector is $\lesssim$0.1 μs, in such a short time the correlated photoion is expected to remain in the photoionization region. Thus, the first extraction pulse serves to extract the correlated photoion as well as background ions formed within Δt. The second extraction pulse draws out only background ions formed in the temporal range of 100 ns. The ions arriving at the ion detector are recorded by a multichannel scaler (MCS). The difference of the ion intensities detected due to the first and second extraction pulse represents the true coincidence signal. The coincidence detection cycle is completed in a period of 100 μs. The electron detector will not accept another TPE until the end of the coincidence period.

Fig. 1a shows the PIPECO spectrum for NO^+ in the wavelength region of 1200–1345 Å obtained using the pulsed PIPECO method. The counting time for each data point is 12 s. The NO^+ PIPECO spectrum is in excellent agreement with the TPE spectrum for NO (fig. 1b) except that the electron background present in the TPE spectrum is not discernible in the PIPECO spectrum. The structureless electron background, which increases gradually as the photon energy is increased, is believed to arise from photoelectrons ejected from the exit slit of the monochromator. The NO^+ spectra show that the electron energy resolution achieved is $\approx$30 meV (fwhm) for a wavelength resolution of 1.4 Å (fwhm). The electron energy resolution is expected to be better when a higher wavelength resolution is used.

The pulsed PIPECO method is found to be su-

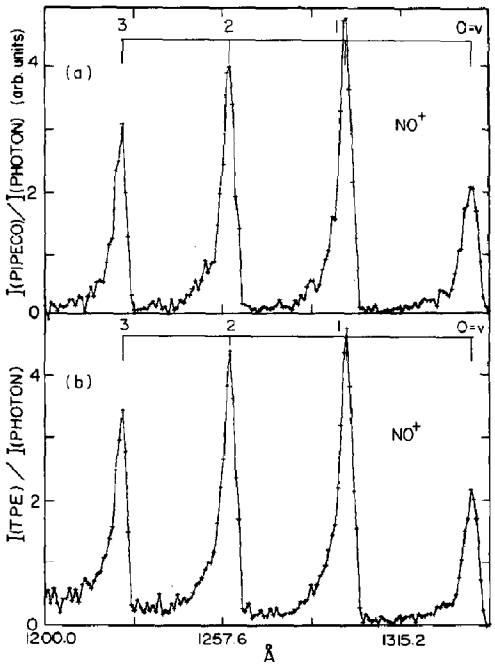

Fig. 1. (a) PIPECO spectrum for NO^+ in the wavelength region of 1200–1345 Å. (b) TPE spectrum for NO^+ in the wavelength region of 1200–1345 Å. (Wavelength resolution = 1.4 Å (fwhm), electron energy resolution $\approx$30 meV (fwhm).)

perior in both sensitivity and resolution compared to the continuous MCS PIPECO scheme [5–7] partly because the electron energy resolution and ion collection efficiency can be optimized in the pulsed PIPECO experiment. The greatest improvement in sensitivity of the pulsed PIPECO method stems from the substantial reduction of false coincidences as a result of the smaller 100 ns temporal window used here compared to the 5–10 μs window determined by the width of the ion time-of-flight peak in the MCS PIPECO experiments. The detailed comparison of the signal-to-noise ratios achieved in the pulsed and MCS PIPECO schemes will be presented in a future publication.

3. Results

Fig. 2 shows the TPE spectrum in the wavelength region of 1030–1210 Å for the gas mixture produced in the discharge of pure SO_2. In this wavelength range, the TPEs result from photoionization of SO, S_2O, S_3, S_2, S, and $O_2(^1\Delta_g)$ etc. The PIE and PIPECO spectra for SO^+ are depicted in figs. 3a and 3b and those for S_2O^+ are compared in figs. 4a and 4b, respectively. The accumulation time for each of the SO^+ and S_2O^+ PIPECO spectra is ≈4 h. The spectra shown in figs. 2 and 3b have been smoothed using a three-point averaging routine. Because of the involvement of autoionization, the PIPECO spectra for SO^+ and S_2O^+ are different from the HeI PESs of SO [8–10] and

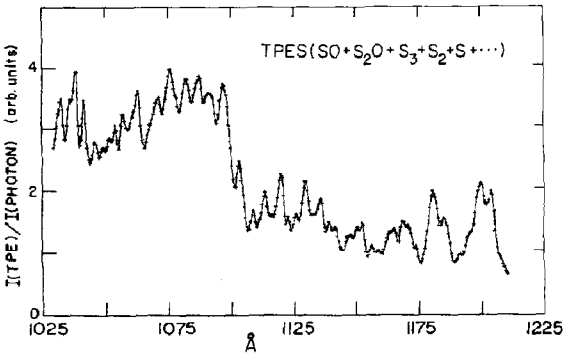

Fig. 2. TPE spectrum for the gas mixture ($SO+S_2O+S_3+S_2+S+...$) produced in the microwave discharge of SO_2 in the wavelength region of 1025–1210 Å. (Wavelength resolution = 1.4 Å (fwhm), electron energy resolution ≈30 meV (fwhm).)

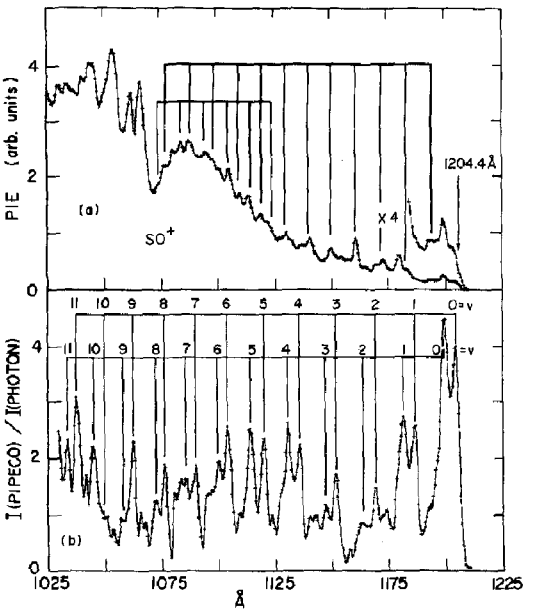

Fig. 3. (a) PIE spectrum for SO^+ in the wavelength region of 1025–1210 Å. (b) PIPECO spectrum for SO^+ in the wavelength region of 1025–1210 Å. (Wavelength resolution = 1.4 Å (fwhm), electron energy resolution ≈30 meV (fwhm).)

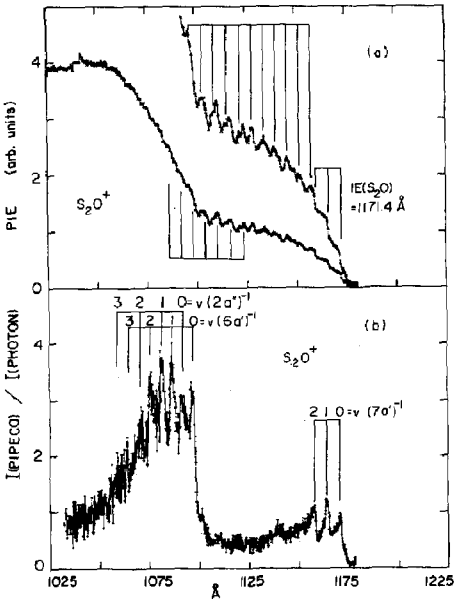

Fig. 4. (a) PIE spectrum for S_2O^+ in the wavelength region of 1025–1180 Å. (b) PIPECO spectrum for S_2O^+ in the wavelength region of 1025–1180 Å. (Wavelength resolution = 1.4 Å (fwhm), electron energy resolution ≈30 meV (fwhm).)

S_2O [11,12]. The PIE spectrum for S_2O shown in fig. 4a is consistent with that reported previously [13].

4. Discussion

4.1. SO

The adiabatic ionization energy (IE) for SO to $SO^+(\tilde{X}\ ^2\Pi_{3/2})$ determined by the SO^+ PIE spectrum is 10.294 ± 0.004 eV (1204.4 ± 0.5 Å) [#2], in agreement with values obtained from the HeI PES of SO [9,10]. The PIE spectrum for SO^+ exhibits complex autoionization features. It appears that most of these features can be grouped into two progressions of vibrational bands with vibrational spacings ($\Delta\tilde{\nu}$) of ≈ 800 cm^{-1} as indicated by tic marks in fig. 3a. The $\tilde{a}\ ^4\Pi$ electronic band observed in the HeI PES of SO consists of a long vibrational progression with an average $\Delta\tilde{\nu}$ value of 750–800 cm^{-1} [9,10]. It is most likely that the progressions resolved in the SO^+ PIE spectrum are due to Rydberg states converging to $SO^+(\tilde{a}\ ^4\Pi)$.

The vertical IE for SO observed in the SO^+ PIPECO spectrum is 10.305 eV. The two peaks in the PIPECO spectrum at wavelengths > 1176 Å are similar to those observed in the HeI PES of SO. The doublet structures of the two peaks have been assigned to the formation of $SO^+(\tilde{X}\ ^2\Pi_{3/2,1/2}, v=0,1)$. Following this assignment, we have been able to assign most of the other peaks in the SO^+ PIPECO spectrum to $SO^+(\tilde{X}\ ^2\Pi_{3/2,1/2}, v=2\text{–}11)$. The assignments summarized in table 1 indicate that the spin–orbit splitting ($\Delta\tilde{\nu}_{sp}$) for the $\tilde{X}\ ^2\Pi$ state is 371 ± 20 cm^{-1}. The uncertainty for this value is mainly contributed by the finite wavelength interval used in the experiment. The $\Delta\tilde{\nu}_{sp}$ value determined here is in agreement with previous measurements [9,10] and the predicted value of 360 cm^{-1} [10,14,15]. Combining the values for the adiabatic IE for SO to $SO^+(\tilde{X}\ ^2\Pi_{3/2})$ and $\Delta\tilde{\nu}_{sp}$, we calculated a value of 10.340 ± 0.005 eV for the adiabatic IE for SO to $SO^+(^2\Pi_{1/2})$.

The vibrational bands observed for SO^+ ($\tilde{X}\ ^2\Pi_{3/2,1/2}$, $v=3\text{–}11$) are the results of autoionization. Based on the observation of the SO^+ ($\tilde{X}\ ^2\Pi_{3/2,1/2}$, $v=0\text{–}3$) PIPECO bands, the average

[#2] This value is determined from a PIE spectrum measured using a wavelength resolution of 0.28 Å (fwhm).

Table 1
Progressions of vibrational bands for $SO^+(^2\Pi_{3/2,1/2}, v=0\text{–}11)$

v	$\tilde{X}\ ^2\Pi_{3/2}$		$^2\Pi_{1/2}$		$\Delta\tilde{\nu}_{sp}$ (cm^{-1}) [c]
	$\tilde{\nu}$ (cm^{-1}) [a]	$\Delta\tilde{\nu}$ (cm^{-1}) [b]	$\tilde{\nu}$ (cm^{-1}) [a]	$\Delta\tilde{\nu}$ (cm^{-1}) [b]	
0	83119		83500		381
		1262		1260	
1	84381		84760		379
		1265		1254	
2	85646		86014		368
		1265		1277	
3	86911		87291		380
		1226		1236	
4	88137		88527		390
		1260		1232	
5	89397		89759		362
		1257		1266	
6	90654		91025		371
		1207		1217	
7	91861		92242		381
		1197		1164	
8	93058		93406		348
		1184		1192	
9	94242		94598 [d]		356
		1169		1178	
10	95411 [d]		95776		365
		1151		1161	
11	96562		96937		375
		$\Delta\tilde{\nu}_{av} = 1222$ [e]		$\Delta\tilde{\nu}_{av} = 1222$ [e]	$\Delta\tilde{\nu}_{sp} = 371 \pm 20$ [f]

[a] Peak positions of vibrational bands. Estimated uncertainty = ± 20 cm^{-1}.
[b] Vibrational spacings. [c] Spin–orbit splitting for $SO^+(\tilde{X}\ ^2\Pi)$. [d] Estimated value.
[e] Average value for $\Delta\tilde{\nu}$. [f] Average value for $\Delta\tilde{\nu}_{sp}$.

Table 2
Progressions of vibrational bands for S_2O^+ ($7a'^{-1}$, $6a'^{-1}$, and $2a''^{-1}$)

v	$\tilde{X}(7a'^{-1})$		$(6a'^{-1})$		$(2a''^{-1})$	
	$\tilde{\nu}$ (cm^{-1}) [a]	$\Delta\tilde{\nu}$ (cm^{-1})	$\tilde{\nu}$ (cm^{-1}) [a]	$\Delta\tilde{\nu}$ (cm^{-1})	$\tilde{\nu}$ (cm^{-1}) [a]	$\Delta\tilde{\nu}$ (cm^{-1})
0	85426	485	91091	922	91558	915
1	85911	475	92013	924	92473	915
2	86386		92937		93388	
		$\Delta\tilde{\nu}_{av}\approx 480$ [b]		$\Delta\tilde{\nu}_{av}=923$ [b]		$\Delta\tilde{\nu}_{av}=915$ [b]

[a] Estimated uncertainties $=\pm 20$ cm^{-1}. [b] Average value for $\Delta\tilde{\nu}$.

value for is 1264 cm^{-1} which is nearly 100 cm^{-1} lower than that reported by Dyke et al. [9]. Nevertheless, the average $\Delta\tilde{\nu}$ value of 1270 ± 20 cm^{-1} observed by Lee [10] is in excellent agreement with the result of this study. The $\Delta\tilde{\nu}$ value decreases from ≈ 1270 to 1150 cm^{-1} as v increases in the range of 0–11. The observed trend of $\Delta\tilde{\nu}$ is consistent with a value of ≈ 5.5 cm^{-1} for the anharmonicity constant.

4.2. S_2O

The value of 10.584 ± 0.005 eV (1171.4 ± 0.5 Å) (see footnote 2) for the adiabatic IE of S_2O to $S_2O^+(X\,^2A')$ determined by the S_2O^+ PIE spectrum agrees with that obtained in the previous PIE study [13]. However, this value is higher than those found in the HeI photoelectron spectroscopic measurements [11,12]. The S_2O^+ PIE spectrum shows two vibrational steps at the onset. The spacings of these steps are equal to the average $\Delta\tilde{\nu}$ value of 480 cm^{-1} observed in the first electronic band of the HeI PES of S_2O. In the wavelength region of ≈ 1090–1157 Å, the S_2O^+ PIE spectrum displays quite regular autoionization features. Some of these features are found to split into doublets in a higher resolution PIE spectrum. The two progressions of autoionization vibrational bands, with spacings of ≈ 480 cm^{-1} indicated in fig. 4a, are consistent with the higher resolution PIE measurement.

The three peaks at wavelengths >1160 Å found in the S_2O^+ PIPECO spectrum, which correspond to the three steps observed in the PIE spectrum, are similar to those in the HeI PES of S_2O [11,12]. These features have been assigned to the formation of $S_2O^+(X\,^2A')$ in the $v_3=0$, 1, and 2 vibrational states. The ν_3 vibrational mode corresponds mainly to S–S stretch. The S_2O^+ PIE and PIPECO spectra rise markedly in the wavelength region of ≈ 1075–1100 Å, indicating the existence of a new electronic band. According to the HeI photoelectron spectroscopic study of Frost et al., the IEs for S_2O to the first $S_2O^+(^2A')$ and second $S_2O^+(^2A'')$ excited states are 11.25 and 11.31 eV and the ν_1 vibrational frequencies of 930 and 940 cm^{-1}, respectively. Using these values, we have assigned the vibronic bands observed in the wavelength region of 1060–1105 Å in fig. 4b to the formation of $S_2O^+(^2A', v_1=0$–$3)$ and $S_2O^+(^2A'', v_1=0$–$3)$. Table 2 summarizes the assignments of the observed vibrational bands for the ground $X\,^2A'$ and the first ($^2A'$) and second ($^2A''$) excited states of S_2O^+. The $\Delta\tilde{\nu}$ values for these states determined here and from the HeI PES of S_2O are in agreement.

5. Conclusion

Using the pulsed PIPECO method described in this report, we have measured the PIPECO spectra for SO and S_2O formed in a discharge of SO_2 in the wavelength region of 1025–1210 Å. The PIE and PIPECO spectra for SO^+ and S_2O^+ have provided accurate energetic and spectroscopic data for these ions. Experiments to extend the PIPECO measurements of S_2O and SO to higher photon energies and to other transient molecules are in progress. This experiment has demonstrated that the pulse PIPECO scheme provides good sensitivity and resolution and is a promising method for the study of radicals coexisting with other molecular species.

References

[1] D.W. Turner, C. Baker, A.D. Baker and C.R. Brundle, Molecular photoelectron spectroscopy (Wiley, New York, 1970).
[2] K. Kimura, S. Katsumata, Y. Achiba, T. Yamazaki and S. Iwata, Handbook of HeI photoelectron spectra of fundamental organic molecules (Halsted Press, New York, 1981).
[3] J.M. Dyke, N. Jonathan and A. Morris, in: Electron spectroscopy, theory, techniques, and applications, Vol. 3 (Academic Press, New York, 1979) p. 189.
[4] P.W. Schenik, Z. Anorg. Allg. Chem. 211 (1933) 150.
[5] K. Norwood, J.-H. Guo, G. Luo and C.Y. Ng, J. Chem. Phys. 88 (1988) 4098.
[6] K. Norwood, J.-H. Guo, G. Luo and C.Y. Ng, Chem. Phys. 129 (1989) 109.
[7] K. Norwood, J.-H. Guo and C.Y. Ng, J. Chem. Phys., in press.
[8] N. Jonathan, K.J. Ross and D.J. Smith, Chem. Phys. Letters 9 (1971) 217.
[9] J.M. Dyke, L. Golob, N. Jonathan, A. Morris, M. Okuda and D.J. Smith, J. Chem. Soc. Faraday Trans. II 70 (1974) 1818.
[10] S.T. Lee, Ph.D. Thesis, The University of British Columbia (1974).
[11] D.C. Frost, S.T. Lee and C.A. McDowell, Chem. Phys. Letters 22 (1973) 243.
[12] H. Bock, B. Solouki, P. Rosmus and R. Steudel, Angew. Chem. 85 (1973) 987.
[13] J. Berkowitz, J.H.D. Eland and E.H. Appelman, J. Chem. Phys. 66 (1977) 2183.
[14] S. Leach, Acta Phys. Polon. 34 (1968) 705.
[15] F.A. Grimm, J. Electron Spectry. 2 (1973) 475.